# Pair tunneling, phase separation and dimensional crossover in imbalanced fermionic superfluids in a coupled array of tubes

Kuei Sun and C. J. Bolech
*Department of Physics, University of Cincinnati, Cincinnati, Ohio 45221-0011, USA*
(Dated: November 21, 2012)

We study imbalanced fermionic superfluids in an array of one dimensional tubes at the incipient dimensional crossover regime, wherein particles can tunnel between neighboring tubes. In addition to single-particle tunneling (ST), we consider pair tunneling (PT) that incorporates the interaction effect during the tunneling process. We find that with an increase of PT strength, a system of low global polarization evolves from a structure with a central Fulde-Ferrell-Larkin-Ovchinnikov (FFLO) state to one with a central BCS-like fully-paired state. For the case of high global polarization, the center region exhibits pairing zeros embedded in a fully-paired order. In both cases, PT enhances the pairing gap, suppresses the FFLO order and leads to spatial separation of fully-paired and fully-polarized regions, same as in higher dimensions. Thus, we show that PT rather than ST is essential for the development of signatures characteristic of the incipience of the dimensional crossover.

PACS numbers: 37.10.Jk, 67.85.Lm, 71.10.Pm

Superconductivity and ferromagnetism are two ubiquitous but competing phenomena in condensed matter systems. Spin imbalance and magnetic field induced by ferromagnetism tend to suppress Cooper pairing, which is responsible for superconductivity. For more than four decades an interesting phase, the Fulde-Ferrell-Larkin-Ovchinnikov (FFLO) state [1, 2], has been suggested as the concurrence of both ferromagnetic and oscillatory superconducting orders [3, 4], but its direct confirmation is still elusive. Recently, owing to the capability of controlling particle densities, tuning interactions and cooling into quantum degeneracy [5, 6], cold atomic systems have become a promising platform for searching for FFLO order [7, 8]. In experiments of trapped Fermi gases, density profiles that reflect the interplay of spin imbalance (ferromagnetic order) and Cooper pairing have been observed [9–11]. In addition, experiments have also revealed significant dimensional dependence of the profiles: in three dimensions (3D) a fully paired profile takes place at the trap center and a polarized profile does off center [9, 10], while in one dimension (1D) the central region is always polarized [11]. These observations agree with theoretical studies of the FFLO state in 1D and the trap-induced phase separation in 3D [12–19], but the marked difference between these two limits also raises the need for understanding the intermediate regime. Several works have focused on the dimensional crossover regime of various kinds of continuous systems [20–25] or Hubbard lattices [26, 27], but with a different emphasis than the present work.

In this paper, we study a realizable system of a two dimensional optical lattice array of 1D tubes, subject to a global trapping potential [11, 28, 29]. The incipient dimensional crossover regime of this system, which can be experimentally accessed by lowering the lattice depth, is modeled by incorporating the kinetics of single-particle tunneling (ST) as well as a key ingredient representing the tunneling of paired opposite-spin atoms – pair tunneling (PT) – between neighboring tubes (as illustrated in Fig. 1). The ST leads to an interesting magnetic compressible-incompressible phase transition analogous to that in the Bose-Hubbard model (discussed in Ref. [25]) but is not responsible for certain observed signatures in the profiles at the dimensional crossover regime (that will be shown below). By considering PT, we are able to describe the evolution of profiles from 1D toward 3D and obtain the emerging signatures of the dimensional crossover at various global polarizations, such as the inversion of the fully-paired and polarized centers as well as the growing spatial separation between the fully-paired and fully-polarized regions. Following, we first discuss the microscopic physical cause of the PT and evaluate its strength using a two-channel model. We then construct a model Hamiltonian and apply a Bogoliubov-de Genne (BdG) treatment to solve for the density and pairing profiles of the system. Finally, we present and discuss the results.

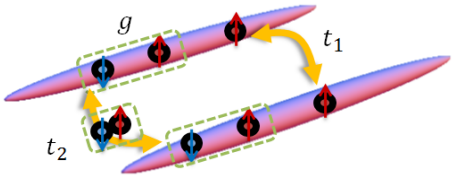


FIG. 1: (color online) Illustration of single particle and pair tunneling processes, $t_1$ and $t_2$, respectively, between two neighboring tubes in the array. On each tube, two opposite-spin atoms can form a bound pair (circled in the graph) in the presence of an attractive interaction $g$. The circled pair in the middle indicates that the two atoms remain paired during the $t_2$ process.

For free fermions in a lattice potential, the inter-site kinetics is well described by ST processes of strength

$t_1$ [30]. For an attractively interacting case where two opposite-spin atoms form a pair of binding energy $\epsilon_b$, the kinetics of the pair tunneling would, in principle, be incorporated as a process in which the two atoms of a pair split, separately tunnel to the other site and re-bind. This is contained in the ST model as a second order process of strength $t_1^2/\epsilon_b$ and accounts for the Josephson phenomena in the presence of superfluid orders, cf. [22].

However, in cold-atom experiments, the interaction is induced via a Feshbach resonance [31], which is controlled by the tuning of a magnetic field affecting the hyperfine energy splittings. Because the field is applied throughout the system, the interaction that leads to pairing exists on and *between* lattice sites. Therefore, we expect that atoms that remain paired during the whole tunneling event can be another viable process (see illustration in Fig. 1). Such process is described as tunneling of the paired atoms, with strength denoted as $t_2$. One can estimate $t_2$ around the Feshbach resonant regime using a two-channel model that incorporates atomic and molecular degrees of freedom (see Appendix). By integrating out the molecular degrees of freedom, we obtain $t_2 = \alpha^2 t_m$, where $t_m$ is the molecular tunneling and $\alpha$ is the ratio of the molecule-atom coupling strength to the molecular chemical potential. Considering the tunneling strength in optical lattices given by $\frac{4}{\sqrt{\pi}} E_R (V_0/E_R)^{3/4} \exp[-2\sqrt{V_0/E_R}]$ with $V_0$ being the optical-lattice depth and $E_R$ being the recoil energy [32], we find $t_2/t_1 = \sqrt{2}\alpha^2 \exp[-2\sqrt{V_0/E_R}]$. This expression shows that the PT effect becomes more important and can even overcome the ST as the lattice depth decreases. In this same limit, perturbative-RG analysis starting from 1D becomes unreliable. In addition, our system shows prevasive pairing effects and is thus different from an array of Josephson junctions that lack the pairing mechanism in the insulating barriers between the superconductors. Therefore, by providing extra channels for Josephson tunneling, the PT processes can lead to an enhancement of the superfluid order and its cross-tube coherence, anticipating the dimensional crossover regime.

Incorporating both the ST and PT effects, the tube lattices occupied by up-spin (majority) and down-spin (minority) atoms, $\hat{\psi}_{\sigma=\uparrow/\downarrow,\mathbf{r}}(z)$, are hence described by the microscopic Hamiltonian

$$\begin{aligned} H &= \int_z \sum_{\mathbf{r}} \big(\sum_\sigma \hat{\psi}^\dagger_{\sigma\mathbf{r}} H^0_\sigma \hat{\psi}_{\sigma\mathbf{r}} - g\hat{\psi}^\dagger_{\uparrow\mathbf{r}}\hat{\psi}^\dagger_{\downarrow\mathbf{r}}\hat{\psi}_{\downarrow\mathbf{r}}\hat{\psi}_{\uparrow\mathbf{r}}\big) \\ &+ \int_z \sum_{\langle\mathbf{r}\mathbf{r}'\rangle} \big(-t_1 \sum_\sigma \hat{\psi}^\dagger_{\sigma\mathbf{r}'}\hat{\psi}_{\sigma\mathbf{r}} - t_2 \hat{\psi}^\dagger_{\uparrow\mathbf{r}'}\hat{\psi}^\dagger_{\downarrow\mathbf{r}'}\hat{\psi}_{\downarrow\mathbf{r}}\hat{\psi}_{\uparrow\mathbf{r}}\big), \quad (1) \end{aligned}$$

with the $\hat{z}$ direction along the tube's axis and $\mathbf{r} = (x, y)$ denoting tube indexes in the plane perpendicular to $\hat{z}$. The one-particle Hamiltonian, $H^0_\sigma = -(\hbar^2/2m)\partial_z^2 + m(\omega_r^2 r^2 + \omega z^2)/2 - \mu_\sigma$, includes the kinetic energy in the $\hat{z}$ direction, the global trapping potential and the spin-dependent chemical potentials. The on-tube atomic coupling, $g$ (taken positive for attractive interaction), is for the 1D-tube limit [33]. The ST (PT) of strength $t_1$ ($t_2$), takes place between nearest-neighbor tubes, $\langle\mathbf{r}\mathbf{r}'\rangle$.

Applying the BdG mean-field theory [34], (which has successfully described tube lattices without PT [25] and a variety of tube confinements [12, 15, 19, 21, 35, 36]), we construct a mean-field Hamiltonian, $H_{\rm M}$, by correspondingly replacing the quartic operators in Eq. (1) with quadratic ones coupled to three different mean fields,

$$\begin{aligned} H_{\rm M} &= \int_z \sum_{\mathbf{r}} \big[\sum_\sigma \hat{\psi}^\dagger_{\sigma\mathbf{r}}\big(H^0_\sigma + U_{\sigma\mathbf{r}}\big)\hat{\psi}_{\sigma\mathbf{r}} \\ &+ \big(\Delta_{\mathbf{r}}\hat{\psi}^\dagger_{\uparrow\mathbf{r}}\hat{\psi}^\dagger_{\downarrow\mathbf{r}} + \text{H.c.}\big)\big] + \int_z \sum_{\langle\mathbf{r}\mathbf{r}'\rangle,\sigma} \mathcal{T}_{\sigma\mathbf{r}\mathbf{r}'}\hat{\psi}^\dagger_{\sigma\mathbf{r}'}\hat{\psi}_{\sigma\mathbf{r}} \quad (2) \end{aligned}$$

Here the Hartree field, $U_{\sigma\mathbf{r}}(z)$, and the BCS gap field, $\Delta_{\mathbf{r}}(z)$, are standard variational fields in previous BdG studies. We introduce a tunneling field, $\mathcal{T}_{\sigma\mathbf{r}\mathbf{r}'}(z)$, as a new ingredient to describe the effective tunneling under the influence of both $t_1$ and $t_2$. We rotate $H_{\rm M}$ into the quasiparticle basis, $\hat{\gamma}_n$, through a Bogoliubov transformation, $\hat{\psi}_{\sigma\mathbf{r}}(z) = \sum_n [u_{n\sigma\mathbf{r}}(z)\hat{\gamma}_{n\sigma} - \sigma v^*_{n\sigma\mathbf{r}}(z)\hat{\gamma}^\dagger_{n,\bar{\sigma}}]$ (where $\bar{\sigma} = -\sigma$), and derive extended BdG equations for the quasiparticle wave functions, $u_{n\sigma}$ and $v_{n\sigma}$, as well as the corresponding energies, $\epsilon_{n\sigma}$. The condition, $\delta\langle H - TS\rangle = 0$, which guarantees solutions of an equilibrium state at temperature $T$, leads to the self-consistent relations,

$$U_{\sigma\mathbf{r}} = -g\left\langle\hat{\psi}^\dagger_{\bar{\sigma}\mathbf{r}}\hat{\psi}_{\bar{\sigma}\mathbf{r}}\right\rangle = -g\sum_n |u_{n\bar{\sigma}\mathbf{r}}|^2 f_{n\sigma}, \quad (3)$$

$$\begin{aligned} \Delta_{\mathbf{r}} &= -g\left\langle\hat{\psi}_{\downarrow\mathbf{r}}\hat{\psi}_{\uparrow\mathbf{r}}\right\rangle - t_2 {\sum_{\mathbf{r}'}}' \left\langle\hat{\psi}_{\downarrow\mathbf{r}'}\hat{\psi}_{\uparrow\mathbf{r}'}\right\rangle \\ &= \sum_n \left(-g u_{n\uparrow\mathbf{r}} v^*_{n\downarrow\mathbf{r}} - t_2 {\sum_{\mathbf{r}'}}' u_{n\uparrow\mathbf{r}'} v^*_{\downarrow n\mathbf{r}'}\right) f_{n\uparrow}, \quad (4) \end{aligned}$$

$$\begin{aligned} \mathcal{T}_{\mathbf{r}\mathbf{r}'\sigma} &= -t_1 - t_2\left\langle\hat{\psi}^\dagger_{\bar{\sigma}\mathbf{r}'}\hat{\psi}_{\bar{\sigma}\mathbf{r}}\right\rangle \\ &= -t_1 - t_2\sum_n u^*_{n\bar{\sigma}\mathbf{r}'} u_{n\bar{\sigma}\mathbf{r}} f_{n\bar{\sigma}}, , \quad (5) \end{aligned}$$

where $f_{n\sigma} = [\exp(\epsilon_{n\sigma}/k_B T) + 1]^{-1}$ is the Fermi distribution function and $\sum'_{\mathbf{r}'}$ runs over all tubes at $\mathbf{r}'$ next to $\mathbf{r}$. Equation (4) shows that the magnitude of the pairing gap is enhanced by $t_2$ in uniform lattices where $\langle\hat{\psi}_{\downarrow\mathbf{r}}\hat{\psi}_{\uparrow\mathbf{r}}\rangle = \langle\hat{\psi}_{\downarrow\mathbf{r}'}\hat{\psi}_{\uparrow\mathbf{r}'}\rangle$ (and would also be in trapped systems, as expected through a local density approximation argument). This enhancement tends to stabilize the fully paired phase against being invaded by unpaired majority atoms; in analogy to the Meissner effect [37] which prevents the superconducting bulk from being penetrated by the magnetic field. When $t_2 = 0$, $\mathcal{T} = -t_1$ turns Eq. (2) back to that for the Hamiltonian with only ST (discussed in Ref. [25]). We numerically solve the BdG equation and apply the solutions to calculate the spatial profiles of pairing gap $\Delta$, total density $\rho = \rho_\uparrow + \rho_\downarrow$, and

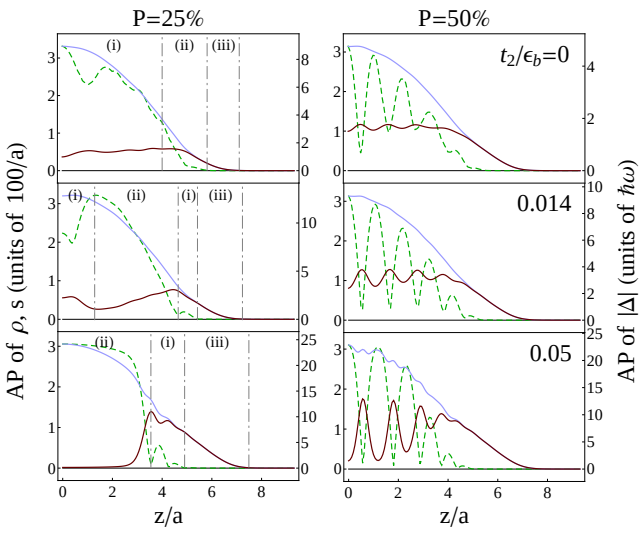


FIG. 2: (color online). Axial profiles (AP) of total density $\rho$, spin imbalance $s$, (solid light blue and dark red curves, respectively, axis on the left of graph), and average magnitude of pairing gap $|\Delta|$ (dashed green curve, axis on the right of graph) for various pair-tunneling strengths $t_2$, and global polarizations $P$. Rows from top to bottom correspond to $t_2 = 0$, $0.014\epsilon_b$, and $0.05\epsilon_b$, respectively; while the left and right columns correspond to $P = 0.25$ and 0.5, respectively. On the left column the dash-dotted lines demarcate regions of (i) FFLO, (ii) BCS-like fully-paired, and (iii) fully-polarized states. The data obtained were for systems of 2400 particles in a $10 \times 10$ tube array with global trapping frequency $\omega = 0.0625\epsilon_b/\hbar$ (which defines the oscillator length, $a$), single particle tunneling $t_1 = 0.014\epsilon_b$, and temperature $T = 0.1\epsilon_b$. These parameters are similar to those used in experiments.

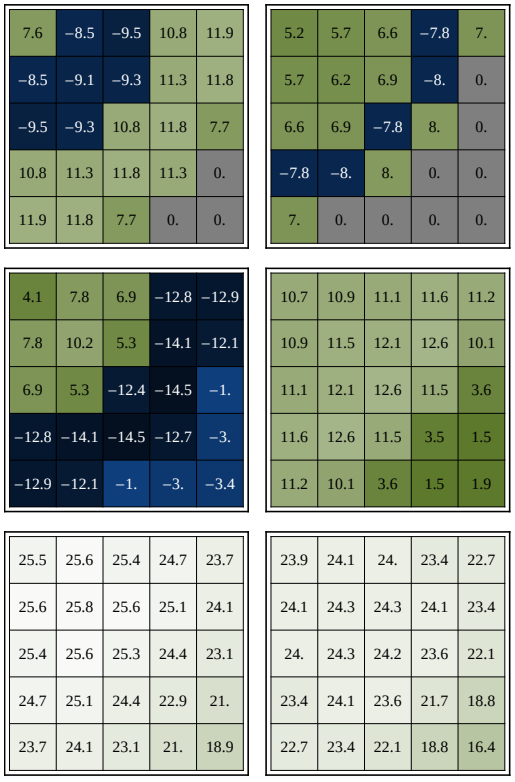


FIG. 3: (color online). Value of the gap function (in units of $\hbar\omega$) at the center of each tube ($z = 0$) for various $t_2$ and $P$ (convention as presented in Fig. 2). Here we show data for $5 \times 5$ tubes in the fourth quadrant of the $10 \times 10$ tube array, in which the top left entry of each panel corresponds to the most central tube. The other quadrants are similar due to 4-fold rotational symmetry.

spin imbalance (or magnetization) $s = \rho_\uparrow - \rho_\downarrow$; where $\rho_\sigma = \langle\hat{\psi}^\dagger_\sigma\hat{\psi}_\sigma\rangle$ is the density profile of $\sigma$ species. Below we present the results for a spherically trapped system ($\omega_r = \omega$).

We look at the influence of $t_2$ at fixed $t_1 = 0.014\epsilon_b$, the latter corresponding to a typical lattice depth of $7E_R$ and thus into the dimensional crossover regime. In Fig. 2, we plot the axial profiles of $\rho$, $s$ and the average of $|\Delta|$ by tracing out the $\mathbf{r}$ degree of freedom. The first and second columns correspond to a lower global polarization of $P = 25\%$ (LP) and a higher one of $P = 50\%$ (HP), respectively [44]. From top to bottom rows, $t_2$ is chosen to be either zero, comparable to $t_1$, or large compared with $t_1$, respectively. We see that in the LP case at $t_2 = 0$, the axial profile exhibits (i) an FFLO center with oscillatory $\Delta$, (ii) a BCS-like shoulder with non-oscillatory $\Delta$, and (iii) a normal tail having zero $\Delta$. At the intermediate $t_2$ value, this tri-layered structure remains. However, the FFLO center shrinks, the BCS-like region extends toward the center accompanied with a drop in imbalance, and the normal tail grows. This indicates a transfer of unpaired majority atoms from the center to the tail. We notice that the gap profile develops small ripples between the BCS-like shoulder [(ii)] and the normal tail [(iii)], suggesting the incipience of an FFLO layer [(i)] here. At the large $t_2$ value, the FFLO center is completely conquered by the BCS-like state and disappears, leaving a large fully-polarized tail and a thin FFLO layer in between them. Because the FFLO and BCS centers are distinctive of 1D [11] and 3D [9, 10] trapped systems, respectively, this result shows the evolution of the system from 1D toward 3D, driven by $t_2$ (compared with increasing $t_1$).

In the HP case, the system always has a center with oscillatory $\Delta$ and a fully-polarized normal tail. In the oscillatory-pairing region, the imbalance profile exhibits characteristic out-of-phase oscillations, with the concurrence of local minima (maxima) of $s$ and local maxima (minima) of $|\Delta|$. This behavior is due to the competition between superfluid and ferromagnetic orders. An increase in $t_2$ enhances this competition, augmenting the magnitude of the out-of-phase oscillations and repelling a portion of the unpaired majority to the normal tail region. At large $t_2$ ($= 0.05\epsilon_b$), the oscillations are large enough that the minima of $s$ are almost zero. Such case

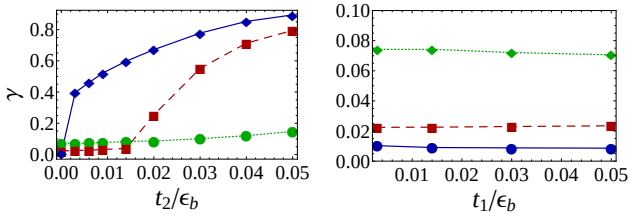


FIG. 4: (color online) The combined fraction of particles in the highly paired ($s/\rho < 5\%$) and highly polarized ($s/\rho > 95\%$) regions, $\gamma$, vs $t_2$ (left panel) or $t_1$ (right panel) with the other fixed. The solid blue, dashed red, and dotted green curves represent cases with global polarization $P = 12.5\%$, 25% and 50%, respectively.

is less like an FFLO state (oscillatory pairing accompanied with finite polarization), but more like spatial alternation of fully-paired superfluid and highly polarized normal gas. This phenomena, analogous to the phase separation in the LP case, is taken as a signature of the dimensional crossover between 1D and 3D at higher polarizations. We also notice that the structure of the profiles is reminiscent of that of a system with vortex cores embedded in a superfluid bulk.

We find that PT affects the pairing order not only along but also across the tubes. Figure 3 shows the value of the gap function at the center of each tube ($z = 0$) in a $10 \times 10$ tube array. The left (right) column corresponds to the LP (HP) case, while, from top to bottom, rows correspond to zero, intermediate, and large $t_2$, respectively (as in Fig. 2). We see that at zero $t_2$ the sign of $\Delta$ changes, indicating an oscillatory behavior across the tubes. In the LP case when $t_2$ increases, the oscillating nodes appear in a more off-center region, as discussed for the axial profiles along the tubes. At large $t_2$, there is no oscillation of $\Delta$ across tubes in both LP and HP cases, showing the suppression of FFLO order. We notice in Figs. 2 and 3 that $t_2$ enhances the maximum magnitude of the gap function, as expected from Eq. (4). This enhancement raises the critical temperature above which the pairing order vanishes and hence agrees with the increase of the superfluid transition temperature in quasi-1D systems [22].

Finally, we look at the phase separation of fully-paired and fully-polarized regions as a function of $t_2$. We consider the combined fraction of particles in the highly paired ($s/\rho < 5\%$) and highly polarized ($s/\rho > 95\%$) regions of the axial profiles; $\gamma \equiv \int_z \rho[\theta(0.05 - s/\rho) + \theta(s/\rho - 0.95)] / \int_z \rho$, where $\theta$ is the step function. The larger $\gamma$ is, the stronger the phase separation the system shows. The left panel in Fig. 4 shows that $\gamma$ monotonically increases with $t_2$ at three various polarizations when $t_1$ is fixed. In the cases of $P = 12.5\%$ and 25% the sudden changes indicate the occurrence of the BCS-like center replacing the FFLO center. For comparison we plot also $\gamma$ vs $t_1$ at fixed $t_2$ in the right panel and observe that $\gamma$ shows almost no change at the three polarizations. This result highlights that it is $t_2$, rather than $t_1$, that accounts for the phase separation and hence is essential for the correct modeling describing the physics at the incipience of the dimensional crossover regime.

In conclusion, considering the microscopic physics of cold atomic systems, we have incorporated both ST and PT processes to effectively model imbalanced fermionic superfluids in an array of 1D tubes at the incipience of the dimensional crossover. Our calculations show that the PT strength is a main factor for the evolution of the system profiles deviating from the 1D limit, which exhibits a central FFLO state, toward the development of 3D signatures, including a central fully-paired state in the LP case and spatial separation between fully-paired and fully-polarized states in both LP and HP cases. These features are reflected in the directly observed density profiles and the pairing orders which can be probed in time-of-flight experiments [38–41]. Our model can be easily generalized to incorporate higher-order, higher-hand or inter-band processes [42, 43], which are expected to be of further help to investigate the system's transition to the continuous 3D limit.

We are grateful to T. Giamarchi for interesting discussions and to the Kavli Institute for Theoretical Physics where these took place (NSF grant No. PHY05-51164). We thank R. Hulet and his group for valuable discussions and the sharing of preliminary experimental data [29]. This work was supported by the DARPA-ARO Award No. W911NF-07-1-0464.

## APPENDIX: EVALUATION OF THE PAIR TUNNELING

In this section we evaluate the PT strength using a two-channel Feshbach resonance model [6, 31]. Interacting fermionic atoms near a Feshbach resonance shall be described using both atomic and molecular degrees of freedom, $\psi_\sigma$ and $\phi$, respectively. In optical lattices, the partition function of the system is

$$\mathcal{Z} = \int D\{\psi_{\sigma i}, \bar{\psi}_{\sigma i}\} D\{\phi_i, \bar{\phi}_i\} \mathrm{e}^{-\int d\tau (S_a + S_m)}, \qquad (6)$$

where $S_a$ contains terms associated only with the atomic degrees of freedom and

$$\begin{aligned} S_m &= -t_m \sum_{\langle ij \rangle, \sigma} \bar{\phi}_i \phi_j - \mu_m \sum_{i,\sigma} \bar{\phi}_i \phi_i \\ &\quad + U_{am} \sum_i \left( \bar{\phi}_i \psi_{\downarrow i} \psi_{\uparrow i} + \text{H.c.} \right) \end{aligned} \qquad (7)$$

involves the molecular tunneling $t_m$, molecular chemical potential $\mu_m$, and the atom-molecule coupling $U_{am}$. Here we assume the molecular interaction is weak such that

the mean-field approximation, $\bar{\phi}_i\bar{\phi}_i\phi_i\phi_i \to \left\langle \bar{\phi}_i\phi_i \right\rangle \bar{\phi}_i\phi_i$, can be applied to incorporate the interaction as effective contributions to the chemical potentials. We integrate out the molecular variable $\phi$ in Eq. (6) and obtain

$$\mathcal{Z} = \int D\{\psi_{\sigma i}, \bar{\psi}_{\sigma i}\} \mathrm{e}^{-\int d\tau (S_a + S'_a)}, \tag{8}$$

where $S'_a$ is expanded as

$$\begin{aligned} S'_a \;=\; & \frac{U_{am}^2}{\mu_m}\Big[ -\sum_i \bar{\psi}_{\uparrow i}\bar{\psi}_{\downarrow i}\psi_{\downarrow i}\psi_{\uparrow i} \\ & -\frac{t_m}{\mu_m}\sum_{\langle ij\rangle,\sigma} \bar{\psi}_{\uparrow i}\bar{\psi}_{\downarrow j}\psi_{\downarrow j}\psi_{\uparrow i} + \mathcal{O}\left(\frac{t_m^2}{\mu_m^2}\right)\Big]. \end{aligned} \tag{9}$$

The first term in Eq. (9) can be treated as an effective inter-atomic interaction, while the second one appears as PT. Therefore, we obtain

$$t_2 = \frac{U_{am}^2}{\mu_m^2} t_m, \tag{10}$$

or $\alpha = U_{am}/\mu_m$ as mentioned before in the text. From Eq. (10) we see that even if the molecular tunneling is smaller than the atomic tunneling ($t_m < t_1$), $t_2$ can be comparable with or even larger than $t_1$ in some parameter regimes. Notice that we focus here on the leading processes in the lowest Bloch band. Incorporating higher-order, higher-hand or inter-band processes is one of the immediate extensions of our model [42, 43].


[1] P. Fulde and R. A. Ferrell, Phys. Rev. **135**, A550 (1964).
[2] A. I. Larkin and Yu. N. Ovchinnikov, Zh. Eksp. Teor. Fiz. **47**, 1136 (1964) [Sov. Phys. JETP **20**, 762 (1965)].
[3] R. Casalbuoni and G. Nardulli, Rev. Mod. Phys. **76**, 263 (2004).
[4] A. I. Buzdin, Rev. Mod. Phys. **77**, 935 (2005).
[5] I. Bloch, J. Dalibard, and W. Zwerger, Rev. Mod. Phys. **80**, 885 (2008).
[6] W. Ketterle and M. W. Zwierlein in *Proceedings of the International School of Physics "Enrico Fermi" in Ultracold Fermi Gases, Course CLXIV, Varenna*, edited by M. Inguscio, W. Ketterle, and C. Salomon (IOS Press, Amsterdam, 2008); see also arXiv:0801.2500.
[7] S. Giorgini, L. P. Pitaevskii, and S. Stringari, Rev. Mod. Phys. **80**, 1215 (2008).
[8] L. Radzihovsky and D. E. Sheehy, Rep. Prog. Phys. **73**, 076501 (2010).
[9] M. W. Zwierlein, A. Schirotzek, C. H. Schunck, and W. Ketterle, Science **311**, 492 (2006).
[10] G. B. Partridge, W. Li, R. I. Kamar, Y.-an Liao, and R. G. Hulet, Science **311**, 503 (2006).
[11] Y.-an Liao, A. S. C. Rittner, T. Paprotta, W. Li, G. B. Partrige, R. G. Hulet, S. K. Baur, and E. J. Mueller, Nature (London) **467**, 567 (2010).
[12] T. Mizushima, K. Machida, and M. Ichioka, Phys. Rev. Lett. **94**, 060404 (2005).
[13] D. E. Sheehy and L. Radzihovsky, Phys. Rev. Lett. **96**, 060401 (2006); Ann. of Phys **322**, 1790 (2006).
[14] G. Orso, Phys. Rev. Lett. **98**, 070402 (2007).
[15] X.-Ji Liu, H. Hu, and P. D. Drummond, Phys. Rev. A **76**, 043605 (2007); Phys. Rev. A **78**, 023601 (2008).
[16] A. E. Feiguin and F. Heidrich-Meisner, Phys. Rev. B. **76**, 220508 (2007).
[17] P. Kakashvili and C. J. Bolech, Phys. Rev. A **79**, 041603(R) (2009).
[18] D.-H. Kim, J. J. Kinnunen, J.-P. Martikainen, and P. Törmä, Phys. Rev. Lett. **106**, 095301 (2011).
[19] L. O. Baksmaty, H. Lu, C. J. Bolech, and H. Pu, Phys. Rev. A **83**, 023604 (2011); New J. Phys. **13**, 055014 (2011).
[20] K. Yang, Phys. Rev. B **63**, 140511(R) (2001).
[21] M. M. Parish, S. K. Baur, E. J. Mueller, and D. A. Huse, Phys. Rev. Lett. **99**, 250403 (2007).
[22] E. Zhao and W. V. Liu, Phys. Rev. A **78**, 063605 (2008).
[23] J. P. A. Devreese, S. N. Klimin and J. Tempere, Phys. Rev. A **83**, 013606 (2011).
[24] R. M. Lutchyn, M. Dzero, and V. M. Yakovenko, Phys. Rev. A **84**, 033609 (2011).
[25] K. Sun and C. J. Bolech, Phys. Rev. A **85**, 051607(R) (2012).
[26] A. E. Feiguin and F. Heidrich-Meisner, Phys. Rev. Lett. **102**, 076403 (2009).
[27] D.-H. Kim and P. Törmä, Phys. Rev. B **85**, 180508(R) (2012).
[28] H. Moritz, T. Stöferle, K. Günter, M. Köhl, and T. Esslinger, Phys. Rev. Lett. **94**, 210401 (2005).
[29] Private communication with R. Hulet.
[30] D. Jaksch and P. Zoller, Annals of Physics **315**, 52 (2005).
[31] C. Chin, R. Grimm, P. Julienne, and E. Tiesinga, Rev. Mod. Phys. **82**, 1225 (2010).
[32] H. P. Büchler, G. Blatter, and W. Zwerger, Phys. Rev. Lett. **90**, 130401 (2003).
[33] M. Olshanii, Phys. Rev. Lett. **81**, 938 (1998).
[34] P. G. De Gennes, *Superconductivity of Metals and Alloys* (Addison-Wesley, Reading, MA, 1989).
[35] K. Sun, J. S. Meyer, D. E. Sheehy, and S. Vishveshwara, Phys. Rev. A **83**, 033608 (2011).
[36] L. Jiang, L. O. Baksmaty, H. Hu, Y. Chen, and H. Pu, Phys. Rev. A **83**, 061604(R) (2011).
[37] W. Meissner and R. Ochsenfeld, Naturwissenschaften **21**, 787 (1933).
[38] T. Kinoshita, T. Wenger, and D. S. Weiss, Science **305**, 1125 (2004); Nature **440**, 900 (2006).
[39] M. Swanson, Y. L. Loh, and N. Trivedi, New J. Phys. **14**, 033036 (2012).
[40] Hong Lu, L. O. Baksmaty, C. J. Bolech, and Han Pu, Phys. Rev. Lett. **108**, 225302 (2012).
[41] C. J. Bolech, F. Heidrich-Meisner, S. Langer, I. P. McCulloch, G. Orso, and M. Rigol, Phys. Rev. Lett. **109**, 110602 (2012).
[42] L.-M. Duan, Phys. Rev. Lett. **95**, 243202 (2005); Europhys. Lett. **81**, 20001 (2008).
[43] C. J. M. Mathy and D. A. Huse, Phys. Rev. A **79**, 063412 (2009).
[44] The global polarization, $P$, is defined as the ratio of total imbalance to the total number of particles. The LP case we focus herein is somewhat higher than the critical polarization of 15–18% verified in experiments.